

Dynamical Instability of a Rotating Dipolar Bose-Einstein Condensate.

R.M.W. van Bijnen^{1,2}, D.H.J. O'Dell³, N.G. Parker¹ and A.M. Martin¹

¹ *School of Physics, University of Melbourne, Parkville, Victoria 3010, Australia.*

² *Eindhoven University of Technology, PO Box 513, 5600 MB Eindhoven, The Netherlands.*

³ *Centre for Cold Matter, Imperial College, Prince Consort Road, London, SW7 2BW, United Kingdom.*

(Dated: July 6, 2018)

We calculate the hydrodynamic solutions for a dilute Bose-Einstein condensate with long-range dipolar interactions in a rotating, elliptical harmonic trap, and analyse their dynamical stability. The static solutions and their regimes of instability vary non-trivially on the strength of the dipolar interactions. We comprehensively map out this behaviour, and in particular examine the experimental routes towards unstable dynamics, which, in analogy to conventional condensates, may lead to vortex lattice formation. Furthermore, we analyse the centre of mass and breathing modes of a rotating dipolar condensate.

PACS numbers: 03.75.Kk, 34.20.Cf, 47.20.-k

In recent years a considerable amount of experimental [1, 2] and theoretical [3, 4, 5, 6, 7, 8, 9, 10, 11] work has been carried out on dilute Bose-Einstein condensates (BECs) in rotating anisotropic traps. Where short-range interactions dominate, a vortex lattice forms when the rotational frequency (Ω) of the system is $\approx 0.7\omega_{\perp}$ (where ω_{\perp} is the trapping frequency perpendicular to the axis of rotation). Insight into the mechanism of vortex formation can be gained by noting that $0.7\omega_{\perp}$ closely coincides with the frequency at which certain hydrodynamic surface excitations become unstable [4, 5]. Through comparison with experimental results [1, 2, 6] and numerical solutions of the Gross-Pitaevskii equation (GPE) [5, 10, 11] such instability has been directly related to the formation of a vortex lattice.

The above results apply to *conventional* BECs composed of atoms of mass m with short-range s-wave interactions, parameterised via $g = 4\pi\hbar^2 a/m$, where a is the s-wave scattering length. However, a recent experiment has formed a BEC of chromium atoms with dipolar interactions [12]. This opens the door to experimentally study the effect of dipolar interactions in BECs. Parallel theoretical work, using a modified GPE, has studied the effect of such long-range interactions on the ground state vortex lattice solutions [13, 14, 15]. However, the route to generating such states has not been explored. For this purpose we solve the hydrodynamic equations of motion for a dipolar BEC in rotating anisotropic harmonic traps. We show that the solutions depend on both the strength of the dipolar interactions, ε_{dd} , and the aspect ratio of the trap, $\gamma = \omega_z/\omega_{\perp}$, in stark contrast to conventional BECs where they are independent of both the strength of the interactions and γ [3, 4]. In addition we evaluate the dynamical stability of our solutions, showing that the region of Ω for which the solutions are stable can be controlled via both ε_{dd} and γ . By analogy to conventional BECs [3, 4, 5], one may expect these instabilities to result in vortex lattice formation in dipolar BECs.

Consider a BEC with long-range dipole-dipole interactions. The potential between dipoles, separated by \underline{r} and aligned by an external electric or magnetic field along a

unit vector \hat{e} is given by, in the notation of Ref. [16],

$$U_{dd}(\underline{r}) = \frac{C_{dd}}{4\pi} \hat{e}_i \hat{e}_j \frac{(\delta_{ij} - 3\hat{r}_i \hat{r}_j)}{r^3}. \quad (1)$$

For low energy scattering of two atoms with dipoles induced by a static electric field $\underline{E} = E\hat{e}$, the coupling constant $C_{dd} = E^2\alpha^2/\epsilon_0$ [17, 18]. Alternatively, if the atoms have permanent magnetic dipoles, d_m , aligned in an external magnetic field $\underline{B} = B\hat{e}$, one has $C_{dd} = \mu_0 d_m^2$ [19]. Denoting ρ as the condensate density, the dipolar interactions give rise to a mean-field potential

$$\Phi_{dd}(\underline{r}) = \int d^3r' U_{dd}(\underline{r} - \underline{r}') \rho(\underline{r}') \quad (2)$$

which can be included in a generalized GPE [18, 19, 20] for the BEC. In the Thomas-Fermi (TF) regime [21] the GPE describing a static dipolar BEC in a harmonic trapping potential $V(\underline{r}) = m(\omega_x^2 x^2 + \omega_y^2 y^2 + \omega_z^2 z^2)/2$ is

$$\mu = \frac{m}{2} (\omega_x^2 x^2 + \omega_y^2 y^2 + \omega_z^2 z^2) + g\rho(\underline{r}) + \Phi_{dd}(\underline{r}), \quad (3)$$

where μ is the chemical potential. For ease of calculation the dipolar potential $\Phi_{dd}(\underline{r})$ can be expressed in terms of a fictitious ‘electrostatic’ potential $\phi(\underline{r})$ [22]

$$\Phi_{dd}(\underline{r}) = -3g\varepsilon_{dd}\hat{e}_i\hat{e}_j \left(\nabla_i \nabla_j \phi(\underline{r}) + \frac{\delta_{ij}}{3} \rho(\underline{r}) \right) \quad (4)$$

where $\phi(\underline{r}) = \int d^3r' \rho(\underline{r}')/(4\pi|\underline{r} - \underline{r}'|)$ and $\varepsilon_{dd} = C_{dd}/3g$ parameterizes the relative strength of the dipolar and s-wave interactions. Self-consistent solutions of Eq. (3) for $\rho(\underline{r})$, $\phi(\underline{r})$ and hence $\Phi_{dd}(\underline{r})$ can be found for any general parabolic trap, see Appendix A of Ref. [22].

We consider atoms trapped in a harmonic potential rotating at a frequency Ω about the z -axis. In the mean field approximation the evolution of the condensate field, $\psi(\underline{r}, t)$, is described by the time-dependent GPE. Writing the condensate field in terms of a density $\rho(\underline{r})$ and a phase $S(\underline{r})$ and neglecting the quantum pressure we obtain the conventional superfluid hydrodynamic equations

$$\frac{\partial \rho}{\partial t} + \nabla \cdot [\rho(\underline{v} - \underline{\Omega} \times \underline{r})] = 0 \quad (5)$$

$$\frac{\partial \underline{v}}{\partial t} + \nabla \left(\frac{\underline{v} \cdot \underline{v}}{2} + \frac{V}{m} + \frac{g\rho}{m} + \frac{\Phi_{dd}}{m} - \underline{v} \cdot [\underline{\Omega} \times \underline{r}] \right) = 0, \quad (6)$$

where $\underline{v} = (\hbar/m)\nabla S$ is the fluid velocity field, in the laboratory frame, expressed in terms of the coordinates in the rotating frame. The stationary solutions of Eqs. (5) and (6) are obtained by imposing the conditions $\partial\rho/\partial t = 0$ and $\partial\underline{v}/\partial t = 0$. We look for solutions of the form [3, 4] $\underline{v} = \alpha(\hat{y}\hat{i} + \hat{x}\hat{j})$, where α is to be determined. We can combine this with Eq. (6) to obtain

$$\mu = \frac{m}{2} (\tilde{\omega}_x^2 x^2 + \tilde{\omega}_y^2 y^2 + \omega_z^2 z^2) + g\rho(\underline{r}) + \Phi_{dd}(\underline{r}) \quad (7)$$

where $\tilde{\omega}_x^2 = \omega_x^2 + \alpha^2 - 2\alpha\Omega$ and $\tilde{\omega}_y^2 = \omega_y^2 + \alpha^2 + 2\alpha\Omega$. The form of Eq. (7) is identical to Eq. (3). Hence we can use the methodology presented in Ref. [22] to calculate $\Phi_{dd}(\underline{r})$. An exact solution of Eq. (7) is given by

$$\rho = n_0 \left(1 - \frac{x^2}{R_x^2} - \frac{y^2}{R_y^2} - \frac{z^2}{R_z^2} \right) \quad \text{for } \rho \geq 0 \quad (8)$$

where n_0 is the central density which is given by normalization to be $n_0 = 15N/(8\pi R_x R_y R_z)$. Following the results presented in Appendix A of Ref. [22] the dipole potential for a polarizing field aligned along the z -axis is

$$\frac{\Phi_{dd}}{3g\varepsilon_{dd}} = \frac{n_0\kappa_x\kappa_y}{2} \left[\beta_0 - \frac{x^2\beta_x + y^2\beta_y + 3z^2\beta_z}{R_z^2} \right] - \frac{\rho}{3} \quad (9)$$

where

$$\beta_k = \int_0^\infty \frac{d\sigma}{(1+\sigma)(\kappa_k^2 + \sigma)\sqrt{(\kappa_x^2 + \sigma)(\kappa_y^2 + \sigma)(1+\sigma)}} \quad (10)$$

with $k = x, y, z$, $\kappa_k = \frac{R_k}{R_z}$ and

$$\beta_0 = \int_0^\infty \frac{d\sigma}{(1+\sigma)\sqrt{(\kappa_x^2 + \sigma)(\kappa_y^2 + \sigma)(1+\sigma)}}. \quad (11)$$

Thus we can rearrange Eq. (7) to obtain the density

$$\rho = \frac{\mu - 3g\varepsilon_{dd}n_0\kappa_x\kappa_y\beta_0 - \frac{m}{2}(\tilde{\omega}_x^2 x^2 + \tilde{\omega}_y^2 y^2 + \tilde{\omega}_z^2 z^2)}{g(1 - \varepsilon_{dd})} \quad (12)$$

where $\tilde{\omega}_{x\{y\}} = \tilde{\omega}_{x\{y\}}^2 - 3\varepsilon_{dd}\kappa_x\kappa_y\beta_{x\{y\}}\omega_z^2/(2\zeta)$, $\tilde{\omega}_z = \omega_z^2(1 - 9\varepsilon_{dd}\kappa_x\kappa_y\beta_z)/(2\zeta)$ and $\zeta = 1 - \varepsilon_{dd}\left[1 - \frac{9\kappa_x\kappa_y}{2}\beta_z\right]$. Comparing the x^2 , y^2 and z^2 terms in Eq. (8) and Eq. (12) we find the three self-consistency relations:

$$\kappa_{x\{y\}}^2 = \left(\frac{\omega_z}{\tilde{\omega}_{x\{y\}}} \right)^2 \frac{1 + \varepsilon_{dd} \left(\frac{3}{2}\kappa_{x\{y\}}^3 \kappa_{y\{x\}} \beta_{x\{y\}} - 1 \right)}{\zeta} \quad (13)$$

and $R_z^2 = \frac{2gn_0}{m\omega_z^2}\zeta$. Now using Eq. (5) in conjunction with Eq. (12) we find the following expression for the stationary solutions to Eq. (5)

$$0 = (\alpha + \Omega) \left(\tilde{\omega}_x^2 - \frac{3}{2}\varepsilon_{dd} \frac{\omega_x^2 \kappa_x \kappa_y \gamma^2}{\zeta} \beta_x \right) + (\alpha - \Omega) \left(\tilde{\omega}_y^2 - \frac{3}{2}\varepsilon_{dd} \frac{\omega_x^2 \kappa_x \kappa_y \gamma^2}{\zeta} \beta_y \right). \quad (14)$$

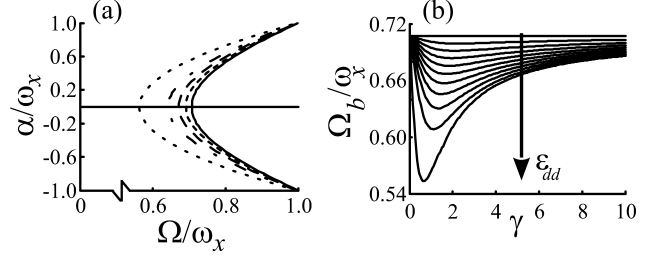


FIG. 1: (a) The irrotational fluid velocity, α , as a function of the trap rotational frequency, Ω , as obtained from Eq. (14), for $\gamma = 1$, $\epsilon = 0$ and $\varepsilon_{dd} = 0$ (solid curve), $\varepsilon_{dd} = 0.25$ (short dashed curve), $\varepsilon_{dd} = 0.5$ (long dashed curve), $\varepsilon_{dd} = 0.75$ (dash dotted curve) and $\varepsilon_{dd} = 0.99$ (dotted curve). (b) The bifurcation point Ω_b versus γ for different dipolar interactions strengths; ε_{dd} increases, in the direction of the arrow, from 0 to 0.9 in steps of 0.1, for the first ten curves, the lowest curve is for $\varepsilon_{dd} = 0.99$.

In the limit $\varepsilon_{dd} = 0$ the solutions of Eq. (14) are independent of g and γ . However, for $\varepsilon_{dd} \neq 0$ the solutions to Eq. (14) are dependent on both the strength of the dipolar interactions and the aspect ratio of the trap.

Introducing the parameter $\epsilon = (\omega_y^2 - \omega_x^2)/(\omega_x^2 + \omega_y^2)$ to define the anisotropy of the trap, we evaluate Eqs. (13) and (14) self-consistently to determine the static solutions of the hydrodynamical equations of motion in the rotating frame. Figure 1(a) shows the solutions to Eq. (14) for various values of ε_{dd} with $\gamma = 1$ and $\epsilon = 0$. For $\varepsilon_{dd} = 0$ (solid curve) we regain the results of Refs. [3, 4] with a bifurcation point at $\Omega_b = \omega_x/\sqrt{2}$ which exactly coincides with the vanishing of the energy of the quadrupolar mode in the rotating frame. For $\Omega < \Omega_b$, one solution, corresponding to $\alpha = 0$, is found. For $\Omega > \Omega_b$, three solutions appear, $\alpha = 0$ and $\alpha = \pm\sqrt{2\Omega^2 - \omega_x^2}/\omega_x$ [3]. The two additional solutions are a consequence of the quadrupole mode being excited for $\Omega \geq \omega_x/\sqrt{2}$. Actually, it is a remarkable feature of the pure s-wave case that these solutions do not depend upon g . This is because in the TF limit surface excitations with angular momentum $\hbar l = \hbar q_l R$, where R is the TF radius and q_l is the quantized wave number, obey the classical dispersion relation $\omega_l^2 = (q_l/m)\nabla_R V$ involving the local harmonic potential $V = m\omega_x^2 R^2/2$ evaluated at R [23]. Consequently $\omega_l = \sqrt{l}\omega_x$, which is independent of g . However, in the case of long-range dipolar interactions the potential Φ_{dd} of Eq. (4) gives non-local contributions, breaking the simple dependence of the force $-\nabla V$ upon R [16]. Thus, we expect the resonant condition for exciting the quadrupolar mode, i.e. $\Omega_b = \omega_l/l$ (with $l = 2$), to change with ε_{dd} . In Fig. 1(a) we see that this is the case: as dipole interactions are introduced, our solutions change and the bifurcation point (Ω_b) moves to lower frequencies.

In contrast to the s-wave case, not only the magnitude of the dipolar coupling ε_{dd} , but also the *shape* of the BEC determines the potential Φ_{dd} . For an oblate ($\kappa_{x,y} > 1$) BEC, more dipoles lie side-by-side, thus giv-

ing a net repulsive interaction, in comparison to the prolate ($\kappa_{x,y} < 1$) case where a majority sit end-to-end, in which configuration the dipolar interaction is attractive. In the extreme limits of $\kappa_{x,y} \rightarrow 0$ and $\kappa_{x,y} \rightarrow \infty$ the angular dependence of the interactions plays no role and the gas behaves conventionally, but in the intermediate regime the role of $\kappa_{x,y}$ and hence the aspect ratio of the trap is important. In Fig. 1(b) we plot Ω_b as a function of γ for various values of ε_{dd} . For $\varepsilon_{dd} = 0$ we find that the bifurcation point remains unaltered at $\Omega_b = \omega_x/\sqrt{2}$ as $\gamma = \omega_z/\omega_x$ is changed [3, 4]. As ε_{dd} is increased the value of γ for which Ω_b is a minimum changes from a trap shape which is oblate ($\gamma > 1$) to prolate ($\gamma < 1$).

Consider now the effect of finite trap anisotropies ($\epsilon > 0$). In Fig. 2(a) we have plotted the solutions to Eq. (14) for various values of ε_{dd} with $\gamma = 1$ and $\epsilon = 0.02$. As in the case without dipolar interactions [3, 4] the solution $\alpha = 0$ is no longer a solution for all Ω . The effect of introducing the anisotropy, in the absence of dipolar interactions, is to *increase* the bifurcation frequency Ω_b . Turning on the dipolar interactions, as in the case of $\epsilon = 0$, *reduces* the bifurcation frequency.

We now analyze two procedures for generating an instability by tracing different paths on Fig. 2(a).

Procedure I: Ω is fixed at $\Omega > \Omega_b(\epsilon = 0)$ and the trap anisotropy is adiabatically turned on. Following analyses for conventional BECs [3, 5, 9] we find that as ϵ is increased adiabatically, from zero, the $\alpha = 0$ solution moves to negative values of α and the BEC follows this route. However, as ϵ is increased further the edge of the lower branch $\Omega_b(\epsilon)$ shifts to higher frequencies. At some critical value of ϵ , $\Omega_b(\epsilon) = \Omega$, the lower branch ceases to be a solution. In this manner the evolution of the static solutions induces instability, which in conventional BECs has been experimentally and theoretically linked to vortex lattice formation [5, 6]. As the dipole interactions are increased the bifurcation frequency is reduced and the range of Ω for which this type of instability can occur increases from $[\omega_x/\sqrt{2}, \omega_x]$ to $[0.5\omega_x, \omega_x]$. In addition, dipolar interactions increase the value of ϵ for which lower branch solutions exist.

Procedure II: ϵ is fixed and Ω is introduced adiabatically. In this case the BEC will follow the upper branch of the solutions. For conventional BECs, a vortex lattice will form [4, 5] when the upper branch solutions ($\alpha > 0$) to Eq. (14) become dynamically unstable. Below we generalize the analysis of Ref. [4] to examine the dynamical stability of the solutions to Eq. (14).

Consider small perturbations in the BEC density and phase of the form $\rho = \rho_0 + \delta\rho$ and $S = S_0 + \delta S$ then, via Eqs. (5, 6) the dynamics of such perturbations can be described, to first order, as

$$\frac{\partial}{\partial t} \begin{bmatrix} \delta S \\ \delta \rho \end{bmatrix} = - \begin{bmatrix} \underline{v}_c \cdot \nabla & \frac{g}{m} (1 + \varepsilon_{dd} K) \\ \nabla \cdot \rho_0 \nabla & [(\nabla \cdot \underline{v}) + \underline{v}_c \cdot \nabla] \end{bmatrix} \begin{bmatrix} \delta S \\ \delta \rho \end{bmatrix} \quad (15)$$

where $K = -3 \frac{\partial^2}{\partial z^2} \int dxdydz / (4\pi |\underline{r}' - \underline{r}|) - 1$ and $\underline{v}_c = \underline{v} - \underline{\Omega} \times \underline{r}$. As in Ref. [4] we consider a polynomial

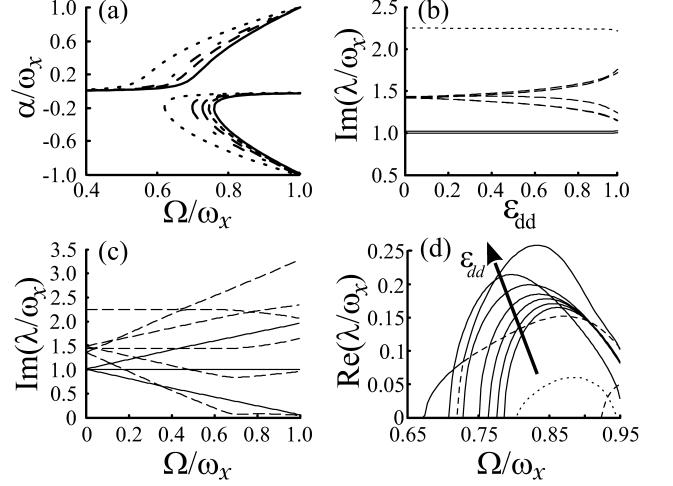


FIG. 2: (a) α vs. Ω , as in Fig 1(a) but for $\epsilon = 0.02$. (b) The positive imaginary eigenvalues of Eq. (15) as a function of ε_{dd} for $\Omega = 0$, $\epsilon = 0.02$, $\gamma = 1$ and $n = 2$. The three solid curves [two at $\text{Im}(\lambda) = \omega_x$ and one at $\text{Im}(\lambda) = \omega_x(1 + \epsilon)^{0.5} = \omega_y$] are the frequencies of the center of mass modes of the BEC. The dashed curves are the frequencies of the breathing modes of the BEC. (c) The positive imaginary eigenvalues of Eq. (15), as a function of Ω for $\varepsilon_{dd} = 0.5$, $\epsilon = 0.02$, $\gamma = 1$ and $n = 2$. The solid (dashed) curves are the frequencies of the center of mass (breathing) modes of the BEC. (d) The maximum positive real eigenvalues of Eq. (15) (solid curves), as a function of Ω , for $\epsilon = 0.02$, $\gamma = 1$, $n = 3$ and $\varepsilon_{dd} = 0, 0.2, 0.4, 0.6, 0.8, 0.95$ and 0.98 ; ε_{dd} increases in the direction of the arrow. The short and long dashed curves are additional positive eigenvalue solutions for $\varepsilon_{dd} = 0.95$ and 0.98 respectively.

ansatz, of order n in the coordinates x, y, z and evaluate the evolution operator for the perturbations. If one or more of the eigenvalues, λ , has a positive real component the stationary solution is dynamically unstable. However, imaginary eigenvalues correspond to stable oscillatory modes of the system [24]. Below we consider both the stable and unstable modes of the upper branch static solutions, for $\gamma = 1$ and $\epsilon = 0.02$.

In Fig. 2(b) we plot the positive imaginary eigenvalues of Eq. (15) for $n = 2$ as a function of the dipolar interaction strength with $\Omega = 0$. As expected we find three modes associated with center of mass oscillations [solid curves in Fig. 2(b)], two at $\text{Im}(\lambda) = \omega_x = \omega_z$ and one at $\text{Im}(\lambda) = \omega_y$. These modes are independent of the strength of the dipolar interactions since they do not alter the shape of the BEC. The higher frequency modes (dashed curves) are associated with the breathing modes of the system [24]. Since these modes do alter the shape of the BEC and the resulting dipolar interactions we find that they are dependent upon ε_{dd} . However, the breathing mode at $\text{Im}(\lambda) = \omega_x\sqrt{5}$ is associated with a perturbation in x, y and z which is equivalent to a uniform re-scaling of the density and as such the frequency of this mode is almost independent of the dipolar interaction strength, as can be seen in Fig. 2(b). Fig. 2(c) shows

how these modes shift as a function of Ω , for $\varepsilon_{dd} = 0.5$. Under the rotation the motion in x and y is coupled. Thus the frequency of the center of mass modes (solid curves) is shifted in the $x-y$ plane [23] whilst remaining constant, at ω_z , in the z direction. Again these modes are independent of the strength of the dipolar interactions. Conversely, the breathing modes (dashed curves) have a relatively complex dependence on ε_{dd} and the rotation frequency.

Finally we consider the real positive eigenvalues of Eq. (15), associated with regions of instability for the upper branch static solutions. In the limit of $\varepsilon_{dd} = 0$ we reproduce Fig. 2 of Ref. [4], with the solutions being unstable in the range $[0.78\omega_x, \omega_x]$ for $\epsilon = 0.02$. In Fig. 2(d) we have plotted the real positive eigenvalues, $\text{Re}(\lambda)$, of Eq. (15), as a function of Ω for various values of ε_{dd} with $n = 3$. For higher values of ε_{dd} [0.95 and 0.98 in Fig. 2(d)] there can be more than one real positive eigenvalue, thus we define the region of instability as the range over which $\max[\text{Re}(\lambda) > 0]$, as shown by the solid curves in Fig. 2(d) [25]. As the dipolar interaction strength is increased the lower bound in Ω for the unstable region is reduced. For example, for $\varepsilon_{dd} = 0.6$ the range of rotation frequencies where the upper branch solution is unstable is $[0.75\omega_x, \omega_x]$, this increases to $[0.67\omega_x, \omega_x]$ for $\varepsilon_{dd} = 0.98$.

By calculating the static hydrodynamic solutions of a rotating dipolar BEC and studying their dynamical stability, we have predicted the regimes of instability of the

condensate. In general we find that the bifurcation frequency, Ω_b , decreases in the presence of dipolar interactions. Thus, for a fixed Ω [at $\Omega > \Omega_b(\epsilon = 0)$] and an adiabatic increase in ϵ , the critical anisotropy at which we expect instability to occur will be higher than for a conventional BEC. Furthermore, we find that the size of this shift not only depends on the strength of the dipolar interactions but also on the aspect ratio of the trap, with the maximal shift being for $\gamma < 1$ ($\epsilon_{dd} \rightarrow 1$). For a fixed anisotropy and an adiabatic increase in Ω we find that as ε_{dd} is increased the lower bound on the rotation frequency at which a rotating dipolar gas will be unstable to perturbations is decreased. In conventional BECs these instabilities have been related to vortex lattice formation [5]. This occurs, primarily, because the instability disrupts the BEC at an Ω which is greater than the rotation frequency at which it is energetically favorable to have a vortex state [26]. However, in a prolate trap the rotational frequency at which it is energetically favorable to form a vortex in a dipolar BEC grows rapidly as ε_{dd} is increased [27] and can exceed the frequency at which we expect an instability to occur. The final state under these circumstances warrants further investigation.

We thank Subhasis Sinha and Yvan Castin for helpful discussions and acknowledge the financial support of the ARC, the EPSRC, the University of Melbourne and QIP IRC (GR/S82176/01).

-
- [1] K.W. Madison, F. Chevy, W. Wohlleben and J. Dalibard, Phys. Rev. Lett. **84**, 806, (2000).
 - [2] E. Hodby *et al.*, Phys. Rev. Lett. **88**, 010405 (2002).
 - [3] A. Recati, F. Zambelli and S. Stringari, Phys. Rev. Lett. **86**, 377 (2001).
 - [4] S. Sinha and Y. Castin, Phys. Rev. Lett. **87**, 190402 (2001).
 - [5] N. G. Parker, R. M. W. van Bijnen and A.M. Martin, Phys. Rev. A **73**, 061603(R) (2006).
 - [6] K.W. Madison, F. Chevy, V. Bretin and J. Dalibard, Phys. Rev. Lett. **86** 4443 (2001).
 - [7] M. Tsubota, K. Kasamatsu and M. Ueda, Phys. Rev. A **65**, 023603 (2002).
 - [8] K. Kasamatsu, M. Tsubota and M. Ueda, Phys. Rev. A **67**, 033610 (2003).
 - [9] E. Lundh, J.-P. Martikainen and K.-A. Suominen, Phys. Rev. A **67**, 063604 (2003).
 - [10] C. Lobo, A. Sinatra and Y. Castin, Phys. Rev. Lett. **92**, 020403 (2004).
 - [11] N. G. Parker and C. S. Adams, Phys. Rev. Lett. **95**, 145301 (2005); J. Phys. B **39**, 43 (2006).
 - [12] A. Griesmaier *et al.*, Phys. Rev. Lett. **94**, 160401 (2005).
 - [13] N.R. Cooper, E.H. Rezayi and S.H. Simon, Phys. Rev. Lett. **95**, 200402 (2005).
 - [14] J. Zhang and H. Zhai, Phys. Rev. Lett. **95** 200403 (2005).
 - [15] S. Yi and H. Pu, Phys. Rev. A **73**, 061602(R) (2006).
 - [16] D.H.J. O'Dell, S. Giovanazzi and C. Eberlein, Phys. Rev. Lett. **92**, 250401 (2004).
 - [17] M. Marinescu and L. You, Phys. Rev. Lett. **81**, 4596 (1998).
 - [18] S. Yi and L. You, Phys. Rev. A **61**, 041604 (2000).
 - [19] K. Góral, K. Rzążewski, and T. Pfau, Phys. Rev. A **61**, 051601 (2000).
 - [20] L. Santos, G.V. Shlyapnikov, P. Zoller, and M. Lewenstein, Phys. Rev. Lett. **85**, 1791 (2000).
 - [21] The limit where the zero-point kinetic energy is negligible compared to the potential and interaction energies.
 - [22] C. Eberlein, S. Giovanazzi and D.H.J. O'Dell, Phys. Rev. A **71**, 033618 (2005).
 - [23] L. Pitaevskii and S. Stringari, *Bose-Einstein Condensation* (Oxford, 2003).
 - [24] Y. Castin, in *Coherent Matter Waves*, Lecture Notes of Les Houches Summer School, edited by R. Kaiser, C. Westbrook and F. David (Springer-Verlag, 2001), p. 1-136.
 - [25] For $n > 3$ we find that although there are more eigenvalues the region of instability, defined by $\max[\text{Re}(\lambda) > 0]$, remains the same.
 - [26] E. Lundh, C.J. Pethick and H. Smith, Phys. Rev. A **55**, 2126 (1997).
 - [27] D.H.J. O'Dell and C. Eberlein, Phys. Rev. A **75**, 013604 (2007).